PCCP

PAPER

View Article Online
View Journal | View Issue

Cite this: *Phys. Chem. Chem. Phys.*, 2015, **17**, 1489

The dynamic crossover in dielectric relaxation behavior of ice I_h

Ivan Popov,[a] Alexander Puzenko,[a] Airat Khamzin[b] and Yuri Feldman*[a]

Received 23rd September 2014,
Accepted 17th November 2014

DOI: 10.1039/c4cp04271a

www.rsc.org/pccp

The main mechanism of the dielectric relaxation process of ordinary hexagonal ice (ice I_h) and its temperature dependence remains unclear. The most interesting and as yet unexplained feature of ice is the presence of the dynamical crossover in relaxation time behavior around T_c = 230 ± 3 K. Since there are no phase transitions in the ice at this temperature (first or second order), we cannot correlate the origin of this crossover with any structural change. Here we present a model according to which the temperature of the crossover is defined by the polarization mechanism. The dielectric relaxation driven by the diffusion of L–D orientational Bjerrum defects (at high temperature, $T > T_c$) is transformed into a dielectric relaxation dominated by the diffusion of intrinsic ionic H_3O^+/OH^- defects (at low temperature, $T < T_c$). In the framework of the model, we propose an analytical equation for the complex dielectric permittivity that takes into account the contribution of both types of defects.

Introduction

Despite the intensive study of electrical properties of ordinary hexagonal ice (ice I_h) over the last century,[1–6] the main relaxation mechanism and its temperature dependence are still unclear. The structural properties of its crystal are well known.[4,7] Namely, each oxygen atom is located at the center of a tetrahedron formed by four other oxygen atoms, separated from one another by about 2.76 Å (see Fig. 1). Unlike the ordered oxygen atoms, the hydrogen atoms are randomly arranged within the crystal in a manner consistent with two Bernal–Fowler–Pauling rules.[3,8,9] Namely, only one hydrogen atom exists on each line connecting the neighboring oxygen atoms. Then, each H_2O molecule is oriented so that its two O–H bonds are directed approximately toward two of the four nearest neighboring oxygen atoms, forming two O–H···O hydrogen bonds. In turn, the oxygen atom of each molecule forms two additional O···H–O hydrogen bonds with one of the other neighboring H_2O molecules. This arrangement leads to an open lattice in which intermolecular cohesion is high. The effect of the Bernal–Fowler–Pauling rules strongly limits the rotational motion of a water molecule in ice.

Dielectric spectroscopy (DS) is an effective spectroscopy tool that allows the study, over a wide range of frequencies and temperatures, of the electric polarization and charge transport in the hydrogen-bond crystals. The results of the first extensive dielectric measurements of H_2O and D_2O ices were reported almost half a century ago by Auty & Cole.[10] Many attempts were made to repeat their measurements during the last few decades,[11–14] however all of these experiments were performed within narrow temperature ranges. The most detailed and accurate dielectric spectroscopy study of H_2O and D_2O ices I_h over wide temperature and frequency ranges was reported by Johari.[15,16] Recently, Shinyashiki *et al.*[17] repeated the measurements for H_2O ice I_h. The main feature of all reported results is the symmetrical broadening of

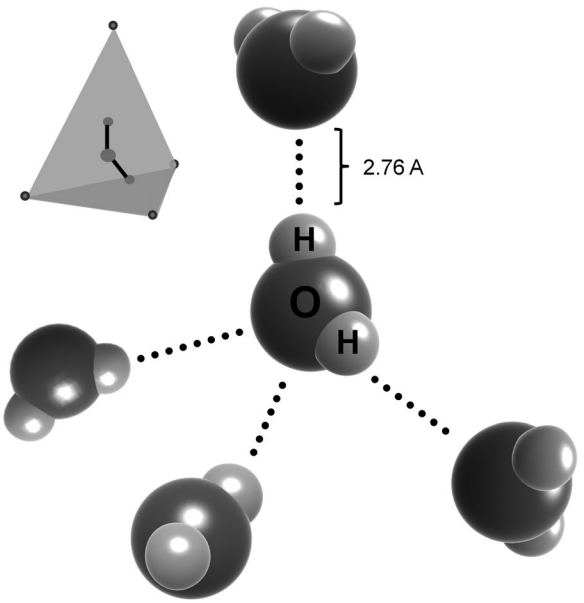

Fig. 1 Orientation of the water molecule in ice lattices.

[a] *The Hebrew University of Jerusalem, Department of Applied Physics, Edmond J. Safra Campus, Givat Ram, Jerusalem 91904, Israel. E-mail: yurif@mail.huji.ac.il*

[b] *Institute of Physics, Kazan (Volga Region) Federal University, Kremlevskaya str.18, Kazan, Tatarstan 420008, Russia*

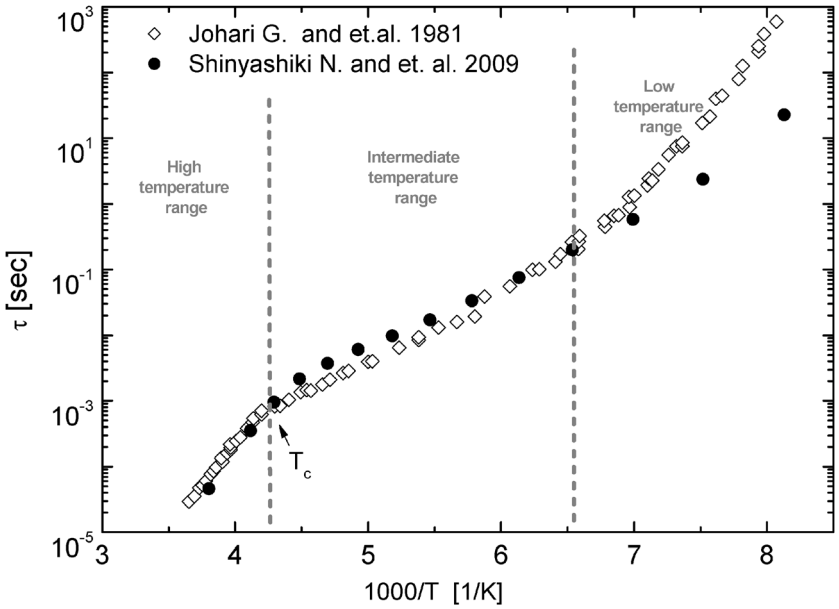

Fig. 2 Experimental data for the temperature dependence of the time relaxation in ice I_h. Open diamonds and full circles denote the data obtained from dielectric spectroscopy studies by Johari[16] and Shinyashiki,[17] respectively. Grey lines are for eye guidance only.

the main loss peak related to ice relaxation, which can be described by the Cole–Cole function $\varepsilon^*(\omega) = \varepsilon_\infty + (\varepsilon_s - \varepsilon_\infty)/(1 + (i\omega\tau)^\alpha)$. The basic properties of each parameter and its temperature dependence have been thoroughly investigated. The parameter ε_∞, which defines the limit value of dielectric permittivity at high frequencies, is almost independent of temperature. The static permittivity ε_s obeys the Curie–Weiss law $\varepsilon_s - \varepsilon_\infty = A/(T - T_{CW})$, where T_{CW} is extrapolated to zero.[16] As for the Cole–Cole parameter α, which defines a broadening of a loss peak (hereinafter CC broadening), experiments on zone-refined single crystals of ice[18] indicate that only a single relaxation time exists above 250 K. Below this temperature, only a small broadening of the peak is observed. In other words, above 250 K the loss peak can be described by the Debye function, *i.e.* $\alpha = 1$, but below this temperature, $\alpha < 1$. Moreover, CC broadening increases with cooling. The values of ice I_h relaxation time obtained by Johari[15,16] and Shinyashiki *et al.*[17] coincide well at the high and intermediate temperature intervals (see Fig. 2). The temperature dependences are described by the Arrhenius law at both intervals with the activation energies of $E_A \approx 53.2$ kJ mol^{-1} and $E_A \approx 18.8 \pm 2$ kJ mol^{-1}, respectively. Moreover, these values concur with previous evaluations.[10–14] At the low temperature interval some deviation exists between these results. If the activation energy increases up to $E_A \approx 46.4$ kJ mol^{-1} as reported in ref. 16, a more recent study[17] also reported a change in activation energy, but not so sharp. Most probably, the results at low temperature depend on the experimental details of the sample preparation and the temperature protocol of the dielectric study. Therefore, we will currently consider only the temperature crossover at $T_c \approx 230 \pm 3$ K.

Regardless of these experimental findings, their theoretical justifications are rather poorly developed.[2–4,19,20] The known models do not take into consideration at all the nature of the CC broadening, *i.e.* the temperature dependence, $\alpha(T)$.

Here, we shall present a model of the dielectric relaxation in ice I_h that explains the crossover temperature at T_c and the variation of the CC spectral broadening parameter α with the temperature.

Dielectric properties of ice I_h in the vicinity of T_c

Let us consider the properties of ice I_h in the vicinity of the crossover temperature. It is known that this crossover coincides approximately with the homogeneous nucleation point of water ($T_N \approx 235$ K), where the phase transition from a supercooled, metastable state of water to crystalline ice takes place. However, at this temperature there is no indication of heat absorption or heat release according to the calorimetric measurements of pure ice I_h.[21] The heat capacity of ice at this temperature behaves monotonically without any jumps. There are also no jumps in the coefficient of thermal expansion, derivatives of heat capacity and derivatives of other thermodynamic potentials. Consequently, there are no first-order phase transitions at T_c. As noted in the Introduction, the static permittivity ε_s obeys the Curie–Weiss law $\varepsilon_s - \varepsilon_\infty = A/(T - T_{CW})$, where T_{CW} tends toward zero.[16] Therefore, no abrupt change occurs in the symmetry at T_c, *i.e.* second-order phase transitions are also not observed in the vicinity of this temperature.

Hence, we can assume that we are dealing with a change in the relaxation mechanisms at this temperature. One of the main features that play a key role in ice dynamics is the hydrogen bond. Moreover, the effect of the Bernal–Fowler–Pauling rules strongly limits the rotational motion of the water molecules in ice.[3]

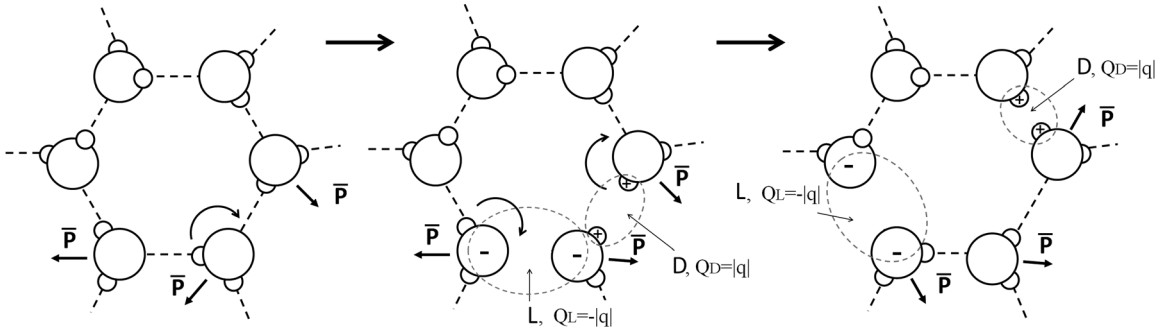

Fig. 3 Schematic representation of the generation and migration of a pair of orientational L- and D-defects in ice I_h with changes in the direction of the dipole moments of water molecules.

Thus, the mechanism of the dielectric relaxation of ice cannot be described by free reorientation of the water molecule. Almost 60 years ago, Bjerrum[22,23] suggested an orientation mechanism for dielectric relaxation and conductivity in ice I_h crystals that has been widely accepted. His model postulated that breaches of the Bernal–Fowler–Pauling rules lead to two kinds of orientational defects D- and L-defects.

According to his theory, a pair of orientational D- and L-defects is formed whenever local thermal excitation forces a H_2O molecule to rotate around one of its O–H···O axes. As a result, one pair of neighboring O···O atoms with no intervening hydrogen (L-defect), and another pair of neighbors O–H H–O with two hydrogen atoms (D-defect) are created. A subsequent similar rotation of one of the adjacent molecules separates these two defects. This process is depicted schematically in Fig. 3. Thus, the reorientation of H_2O molecules can occur only at the defect sites (*i.e.* when defects visit water molecule), which leads to a change in the macroscopic dipole moment. Bjerrum estimated that the energy needed for these defect formations would be approximately equal to the electrostatic lattice energy of ice of $\sim$54.4–56.1 kJ mol^{-1} (see the estimations in ref. 4). However, there have been discussions in the literature that the Bjerrum model, in the simple form presented in Fig. 3, cannot be correct. For example, it was shown by Buch *et al.*,[24] that the electrostatic repulsion between the partial positive charges on the H atoms of the D-defect and between the partial negative charges of the L-defect is bound to alter the defect structure. In this work, the more complicated behavior of L–D defects with different quantum corrections was investigated in detail. Moreover, it is worth mentioning that, besides L–D defects, in ice there may exist other types of orientational defects.[25,26] However, the activation energy of generation and migration of these various orientational defects is around Bjerrum's previous estimations ($\sim$54.4–56.1 kJ mol^{-1}).[24–26] The main parameter for our model is the activation energy of defects. Therefore, for convenience, hereinafter we use the term ''L–D defects'' to represent any possible type of orientational defect.

In addition to orientational defects, the polarization of ice may be driven by the generation of H_3O^+ and OH^- pairs that are also known as ionic defects (see Fig. 4). They are formed in ice when a proton hops from its normal position to one near an adjacent molecule. The resulting 'excess' proton diffuses through the H-bond network *via* the formation or cleavage of covalent bonds, a phenomenon known as proton hopping or the 'Grotthuss mechanism'.[19,27] A similar mechanism is valid for the OH^- defect. The activation energy of proton mobility in ice and liquid water is comparable and roughly equal to 8–13 kJ mol^{-1} (ref. 28 and 29). An additional 10.8 kJ mol^{-1} (ref. 27) is associated with the isotropic electrostatic interaction, leading to a total enthalpy of about 18–23 kJ mol^{-1} per hydrogen bond. This value coincides with the activation energy derived from the dielectric relaxation time in the intermediate temperature region (see Fig. 2 below T_c).

In view of these facts, it seems that the main cause of the activation energy crossover at T_c is transformation of the relaxation mechanism driven by the diffusion of L–D orientational defects to

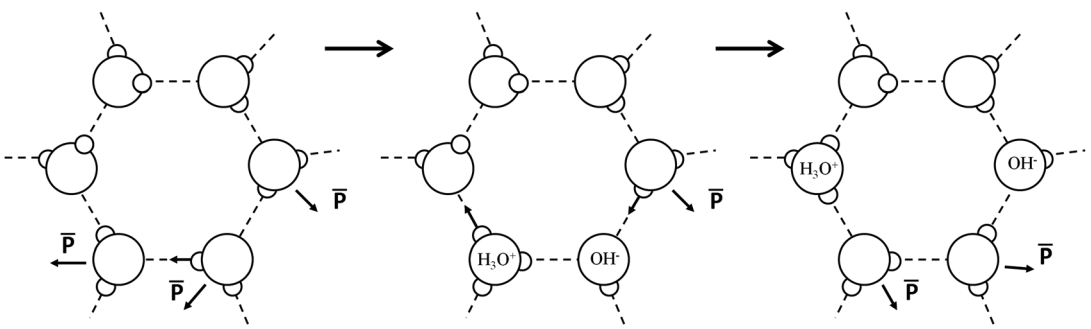

Fig. 4 Schematic representation of the generation and migration of an ionic pair of H_3O^+/OH^- defects in ice I_h with a change in the dipole moment's direction of water molecules.

one where the diffusion of intrinsic ionic H_3O^+/OH^- defects is dominant. A similar explanation has been proposed by Bilgram & Granicher,[20] but has not been disseminated.

An alternative explanation for the activation energy decrease near T_c has been suggested by Gough & Davidson[12] and comprehensively examined in ref. 30. They assigned the E_A alteration at lower temperatures to the presence of impurities and their contribution to the increase in the concentration of orientational defects. Thus, it is likely that a small amount of impurity in ice may produce orientational defects at $T < T_c$ that are greater in number than those produced by the thermal motion of water molecules (intrinsic defects), and thus may cause the activation energy E_A to become appreciably smaller.[12] However, this mechanism cannot explain the spectrum broadening change near T_c. Experimentally, crossover in the CC broadening also corresponds to the crossover in temperature behavior of the time relaxation at T_c.

In this paper we will simultaneously consider both types of defects and their contribution to the mechanism of dielectric relaxation and its temperature dependence in the vicinity of T_c.

The model of the dielectric relaxation in ice I_h

Following the idea of L–D pair and ionic H_3O^+/OH^- defects, we can consider their migration as the main mechanism of dielectric polarization $P(t)$ in ice. Indeed, the additional proton in H_3O^+ ions and the charge hole in OH^- ions can be considered as positive and negative charge carriers, respectively. The similar locally concentrated density of positive charges (D-defects) and negative charges (L-defects) can be assigned to the orientational defects (see Fig. 3). The straying of these defects corresponds with the charge migration. Thus, we can consider the ice structure as a dipole system with charge carriers, where migration of these carriers leads to the total polarization change. If we assume that defect migration is the only cause of the change in polarization $P(t)$, then the Fourier-transform

$$f^*(\omega) = \int_0^\infty f(t)\mathrm{e}^{-i\omega t}\mathrm{d}t,$$

of the relaxation function $\phi(t) = P(t)/P(0)$ can be written as follows (see Mathematical appendix A)

$$\phi^*(\omega) = \frac{1}{i\omega + \sigma_s^*(\omega)/\varepsilon_0}, \quad (1)$$

where

$$\sigma_s^*(\omega) = \sigma_{LD}^*(\omega) + \sigma_\pm^*(\omega), \quad (2)$$

σ_s is the total conductivity caused by the charge transfer due to L–D (σ_{LD}) and ionic H_3O^+/OH^- ($\sigma_\pm$) defects. Note that the different types of carriers are not correlated to one another. According to ref. 31 the frequency-dependent conductivity is determined by the Fourier transform of the mean-squared displacement (MSD) $\langle r^2(t)\rangle$ using

$$\sigma^*(\omega) = -\omega^2\frac{Nq^2}{6k_BT}\lim_{\delta\to 0}\int_0^\infty \langle r^2(t)\rangle \exp(-i\omega t - \delta t)\mathrm{d}t. \quad (3)$$

Here, N is the number density of the mobile carriers, q is the carrier charge, and k_B is the Boltzmann constant. Then, from eqn (3) we have

$$\sigma_s^*(\omega) = \frac{-\omega^2}{6k_BT}\left[N_{LD}q_{LD}^2\langle r^{*2}(\omega)\rangle_{LD} + N_\pm q_\pm^2\langle r^{*2}(\omega)\rangle_\pm\right], \quad (4)$$

where $\langle r^{*2}(\omega)\rangle$ is a one-sided Fourier transform of the mean-squared displacement $\langle r^2(t)\rangle$ of the charge carriers. The random migration of defects from site to site through the H-bond network can be considered as a diffusion process. For normal (Brownian) diffusion the MSD is time-dependent

$$\langle r^2(t)\rangle = Dt, \quad (5)$$

where D is the diffusion coefficient of the random walker in an arbitrary direction.[32] It can be defined using the simple relationship $D = \xi^2/6\tilde{\tau}$, where ξ is the mean hopping distance and $\tilde{\tau}$ is the average time taken to complete a single hop. However, in the general case, the mean-squared displacement becomes nonlinear and must be described as follows:[33–36]

$$\langle r^2(t)\rangle = \frac{\xi^2}{6}\left(\frac{t}{\tilde{\tau}}\right)^\alpha, \quad 0 < \alpha < 1, \quad (6)$$

where the temperature-dependent parameter α defines the degree of deviation from the classical diffusion behavior. Such a sub-diffusive, mean-squared displacement is well known as anomalous diffusion or continuous random walk limited to a fractal geometry.[32] One probable reason for anomalous diffusion is that the defects in ice I_h can only move in a certain direction, namely, only in the direction of the H-bond and their migration outside the network is prohibited.[32] Moreover, due to its quantum mechanical nature, a single hop of proton has only a probabilistic character and the time intervals between the consecutive hops may vary. In other words, MSD of defects is averaged over a time set and can be described by anomalous behavior.[37] The one-sided Fourier transform of eqn (6) is

$$\langle r^{*2}(\omega)\rangle = \frac{\xi^2\Gamma(\alpha+1)(i\omega\tilde{\tau})^{-\alpha}}{6i\omega}, \quad (7)$$

where $\Gamma(x)$ is the gamma function. Assuming that both displacements in eqn (4) have anomalous behavior, we obtain

$$\sigma_s^*(\omega) = \frac{i\omega e^2 l^2}{36k_BT}\left[N_{LD}\Gamma(\alpha_{LD}+1)(i\omega\tilde{\tau}_{LD})^{-\alpha_{LD}} + N_\pm\Gamma(\alpha_\pm+1)(i\omega\tilde{\tau}_\pm)^{-\alpha_\pm}\right]. \quad (8)$$

Here, we have assumed that each L–D or ionic OH^-/OH_3^+ defect charge carrier is equal to the charge of a proton, $q_{LD} = q_\pm = e$, and the mean hopping distance of a carrier is approximately equal to the distance of an O–O link in the ice I_h, $\xi_{LD} = \xi_\pm = l$. The hopping rate is temperature-dependent and for most materials, including ice, it is driven by Boltzmann kinetics in accordance with the Arrhenius law

$$\tilde{\tau}_{LD} = \tilde{\tau}_0^{LD}\exp(E_{LD}/k_BT), \quad \tilde{\tau}_\pm = \tilde{\tau}_0^{\pm}\exp(E_\pm/k_BT), \quad (9)$$

where E_{LD} and $E_\pm$ are the energies of activation for the migration of L–D and ionic OH^-/OH_3^+ defects, respectively; $\tilde{\tau}_0^{LD}$ and $\tilde{\tau}_0^{\pm}$ are free time of a single hop from one site to another.

To obtain the dielectric permittivity $\varepsilon^*(\omega)$ we substitute eqn (8) into eqn (1) and use the following relationship

$$\frac{\varepsilon^*(\omega)-\varepsilon_\infty}{\varepsilon_s-\varepsilon_\infty}=\hat{F}\left[-\frac{d\phi(t)}{dt};i\omega\right]=1-i\omega\phi^*(\omega), \quad (10)$$

where $\hat{F}[\phi(t)]$ is the one-sided Fourier transform of the relaxation function $\phi(t)$. As a result, we obtain

$$\varepsilon^*(\omega)=\varepsilon_\infty+\frac{\Delta\varepsilon}{\left(1+[(i\omega\tau_{LD})^{-\alpha_{LD}}+(i\omega\tau_\pm)^{-\alpha_\pm}]^{-1}\right)}. \quad (11)$$

Here, we denote $\Delta\varepsilon=\varepsilon_s-\varepsilon_\infty$ and

$$\tau_{LD}=\tau_\infty^{LD}\exp(E_{LD}/k_BT),\quad \tau_\pm=\tau_\infty^{\pm}\exp(E_\pm/k_BT), \quad (12)$$

where

$$\tau_\infty^{LD}=\tilde{\tau}_0^{LD}\left[\frac{e^2l^2N_{LD}\Gamma(\alpha_{LD}+1)}{36k_BT\varepsilon_0}\right]^{-1/\alpha_{LD}},$$
$$\tau_\infty^{\pm}=\tilde{\tau}_0^{\pm}\left[\frac{e^2l^2N_\pm\Gamma(\alpha_\pm+1)}{36k_BT\varepsilon_0}\right]^{-1/\alpha_\pm}. \quad (13)$$

An equation similar to eqn (11) has been obtained previously and takes into account the existence of different relaxation channels and their self-similarity.[38–41] This equation has been applied successfully to the glass-formers where the α-relaxation process is followed by an excess wing.[38,39] However, our eqn (11) is derived using the anomalous diffusion of different defects in ice. In the case where the α_{LD} and $\alpha_\pm$ parameter values are close to each other ($|\alpha_{LD}-\alpha_\pm|=\Delta\alpha\ll 1$), eqn (11) presents only one peak (see Mathematical appendix B). The asymmetrical shape of this spectrum, together with the excess wing generated for two values of $\Delta\alpha$, is presented in Fig. 5.

However, the main ice I_h peak shows only a slight broadening without a visible excess wing at the wide temperature interval.[16,18] Thus, in our case, α_{LD} and $\alpha_\pm$ are approximately equal to unity *i.e.* $|\alpha_{LD}-\alpha_\pm|=\Delta\alpha\ll 1$. In this case, the Cole–Cole function provides the best fit, where parameters α and τ are functions of α_{LD}, $\alpha_\pm$, τ_{LD}, and $\tau_\pm$, *i.e.*,

$$\varepsilon^*(\omega)=\varepsilon_\infty+\frac{\Delta\varepsilon}{\left(1+[(i\omega\tau_{LD})^{-\alpha_{LD}}+(i\omega\tau_\pm)^{-\alpha_\pm}]^{-1}\right)}\approx\varepsilon_\infty+\frac{\Delta\varepsilon}{1+(i\omega\tau)^{\alpha}}, \quad (14)$$

where (see Mathematical appendix B)

$$\alpha=\frac{\alpha_{LD}\tau_{LD}^{-\langle\alpha\rangle}+\alpha_\pm\tau_\pm^{-\langle\alpha\rangle}}{\tau_{LD}^{-\langle\alpha\rangle}+\tau_\pm^{-\langle\alpha\rangle}},\quad \langle\alpha\rangle=\frac{\alpha_{LD}+\alpha_\pm}{2}. \quad (15)$$

and

$$\tau=\langle\tau\rangle\left[1+\frac{\alpha-\alpha_\pm}{2\langle\alpha\rangle}\ln(\tau_{LD}/\langle\tau\rangle)+\frac{\alpha-\alpha_{LD}}{2\langle\alpha\rangle}\ln(\tau_\pm/\langle\tau\rangle)\right],$$
$$\langle\tau\rangle=\left[\tau_{LD}^{-\langle\alpha\rangle}+\tau_\pm^{-\langle\alpha\rangle}\right]^{-1/\langle\alpha\rangle}. \quad (16)$$

Eqn (15) and (16) describe the temperature dependence of the Cole–Cole parameter $\alpha(T)$ and time relaxation $\tau(T)$ of ice I_h. Note that in this case the excess wing has been neglected.

Comparison with experiment

Due to the divergence between the experimental data obtained from Johari[16] and Shinyashiki[17] below $T\approx 175$ K, in this work we will only compare the high and intermediate temperature behavior of the relaxation times in ice I_h (up to 175 K). Note that the relaxation time behavior crossover at around $T_c\approx 230\pm 3$ K exists in both experiments. The fit of the experimental data by the CC (eqn (14)) gives the temperature dependence of the relaxation time $\tau(T)$ and parameter $\alpha(T)$, in agreement with the prediction of eqn (15) and (16), where the parameters α_{LD}, $\alpha_\pm$, τ_{LD}, and $\tau_\pm$ are also functions of temperature. However, to describe the experimental behavior presented in Fig. 2, it is enough to assume that $\tau_{LD}(T)$ and $\tau_\pm(T)$ have an Arrhenius temperature behavior (eqn (12)), while the parameters α_{LD} and $\alpha_\pm$ have a weak temperature dependence and can be considered constant. In the framework of such an assumption, it is easy to show that $\tau(T)$ from eqn (16) can be reduced to

$$\tau\approx\langle\tau\rangle=\left[\tau_{LD}^{-\langle\alpha\rangle}+\tau_\pm^{-\langle\alpha\rangle}\right]^{-1/\langle\alpha\rangle}. \quad (17)$$

Here, the balance between the simple sum of two exponential laws defines the crossover temperature as the transition from dominance of the L–D defect mechanism described by $\tau_{LD}(T)$ to dominance of another mechanism defined by $\tau_\pm(T)$. Then, we expect $\alpha(T)$ to exhibit temperature dependence as a step-like function from α_{LD} to $\alpha_\pm$.

Fig. 6 presents the time relaxation fitting and Cole–Cole parameters *versus* temperature, where the relaxation time is adopted from ref. 17 and the CC parameters were evaluated from the experimental spectrum obtained from ref. 42. Here, we have assumed a negligible temperature dependence for $\tau_\infty^{\pm}$ and τ_∞^{LD}, because they are very slow in comparison with the exponent in eqn (12). As can be seen, the fitting functions (15) and (16) describe the experimental data well. The fitting parameters

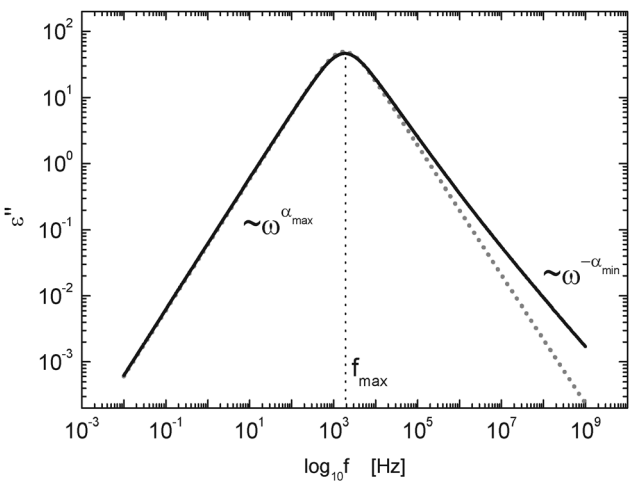

Fig. 5 Model data for dielectric losses (solid line) generated by eqn (11) for values of parameters: $\varepsilon_\infty=3$, $\Delta\varepsilon=100$, $\tau_{LD}=10^{-4}$ s, $\tau_\pm=10^{-3}$ s, (black solid line) $\alpha_{LD}=1$, $\alpha_\pm=0.7$ and (gray short dotted line) $\alpha_{LD}=1$, $\alpha_\pm=0.9$. In these cases $\alpha_{max}=\alpha_{LD}$ and $\alpha_{min}=\alpha_\pm$.

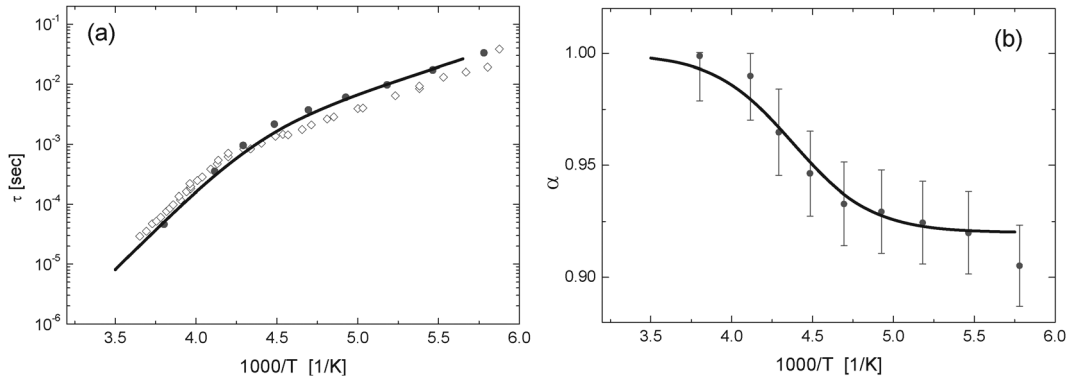

Fig. 6 Fitting of the experimental data to the temperature dependence of (a) the relaxation time and (b) the Cole–Cole parameter. Open diamonds and full circles are the data obtained from dielectric spectroscopy by Johari[16] and Shinyashiki,[17] respectively. In (a) the error bars are defined by the size of the symbols. The black line is the fitting curve by eqn (15) for Shinyashiki's data for high and intermediate temperature ranges.[42]

obtained for the results presented in Fig. 6 are as follows: $\tau_\infty^{\pm} = 3 \times 10^{-7}$ s and $\tau_\infty^{LD} = 2.3 \times 10^{-15}$ s, $E_{LD} \approx 52.4$ kJ mol^{-1} and $E_\pm \approx 17$ kJ mol^{-1} in eqn (12), $\alpha_{LD} \approx 1$ and $\alpha_\pm \approx 0.92$. The fitting parameters E_{LD} and $E_\pm$ coincide with the activation energy of L–D and ionic defects. The significant difference between the values of $\tau_\infty^{\pm}$ and τ_∞^{LD} can easily be explained. Indeed, from eqn (13) it is clear that since α_{LD} and $\alpha_\pm$ are of unity order, we can write $\tau_\infty^{LD}/\tau_\infty^{\pm} \sim N_\pm/N_{LD}$, approximately. It is known[4] that the concentration of orientational defects is about $c_{LD} \approx 10^{-7}$ mole-of-defects/mole of ice and the concentration of ionic defects is $c_\pm \approx 10^{-12}$ mole-of-defects/mole of ice. Thus

$$\frac{\tau_\infty^{LD}}{\tau_\infty^{\pm}} \sim \frac{N_\pm}{N_{LD}} = \frac{c_\pm}{c_{LD}} \approx 10^{-5}, \tag{18}$$

which is in good agreement with the experimental results, and supports our assumption that the origin of the dynamical crossover at $T_c \approx 230 \pm 3$ K is a shift in the relaxation mechanism *via* orientational L–D defects to that of relaxation *via* ionic H_3O^+/OH^- defects. Although the activation energy of the L–D defect migration is higher than that of the ionic defect migration, their overall number exceeds that of the ionic defects. This means that at high temperatures when it is easier to overcome the potential barrier, the probability of a total polarization change by L–D defects is higher due to their large quantity. However, as temperature decreases, it becomes more difficult to overcome the higher barrier, and the probability of dipole polarization shift due to the ionic defects increases. The condition of the crossover temperature $\tau_{LD}(T_c) = \tau_\pm(T_c)$ can be presented as follows:

$$T_c = \frac{E_{LD} - E_\pm}{k_B\left(\ln \tau_\infty^{\pm} - \ln \tau_\infty^{LD}\right)}. \tag{19}$$

Taking into account the fitting values of E_{LD}, $E_\pm$ and $\tau_\infty^{\pm}$, τ_∞^{LD} we obtained $T_c = 228 \pm 5$ *K*, which is in excellent agreement with the experimental observations.

Now we attempt an explanation for the value of the CC parameters: $\alpha_{LD} \approx 1$ and $\alpha_\pm \approx 0.92$. If an ice consists of a regular lattice of water molecules, then the migration of charge carriers through this lattice *via* H-bonds does not lead to delay of its movement in comparison with normal diffusion ($\langle r^2(t)\rangle \sim t$). Therefore, for orientational defects we have $\alpha_{LD} \approx 1$. On the other hand, we may consider the orientational defect as a local break of a H-bond. This local break serves as a restriction for the transport of ionic defects (H_3O^+/OH^-). As a result, at low temperatures, when the L–D defects are not mobile in comparison with the proton hopping (since the energy activation is high), we may consider the ice lattice as non-regular for ionic defect migration. In other words, protons have to bypass the broken H-bonds, spending a considerable amount of time. The trapping of a proton by orientational defects is also possible. This can lead to a deviation from the proton's normal diffusion behavior ($\langle r^2(t)\rangle \sim t^{\alpha}$). According to ref. 32 the parameter α defines the fractal dimension d_f of a geodesic line lying on the fractal set $d_f = 1/\alpha$. Thus for the ionic defects we obtain $d_f^{\pm} = 1/\alpha_\pm = 1.087$.

Conclusion

In summary, we conclude that the origin of the temperature crossover at $T_c \approx 230 \pm 3$ K is not due to the structural transitions in ice, but due to the change in the relaxation mechanism. Therefore, we have defined this crossover as a dynamical one. We have shown that due to the special structure of ice I_h, two possibilities exist for changing its total polarization. The first relaxation mechanism is attributed to the generation and migration of L–D defects, and the second relaxation mechanism is ascribed to the generation and migration of ionic defects. These two mechanisms coexist at any given temperature. However, the L–D defects are dominant in the high temperature interval, while the ionic defects have a greater influence at lower temperatures. The transition between these two mechanisms is revealed as a crossover in the temperature dependence of the relaxation time. Moreover, the model developed can assist greatly in the study of hydrated complex systems where the polarization and relaxation mechanisms can be reduced to the simple problem of random walk.

It is worth noting that the theoretical results, obtained in this work, cannot be directly extended to a deep low temperature range. Eqn (15) and (16) cannot produce the second crossover in

the temperature dependence of the time relaxation (see Fig. 2). Therefore, the model in the present state is applicable only up to beginning of the second crossover (approximately 150 K). Johari in ref. 16 suggested that the second crossover is a transition back to the mechanism of the orientation defects, which is responsible for the high temperature range. It can happen, for example, due to suppression of ionic dissociation. Additionally, it remains unclear whether the way of a sample preparation of ice affects experimental results, namely, in the beginning of the second crossover. Therefore, it is important to verify the experimental details in the low temperature regime, before considering the new models regarding the second crossover.

Mathematical appendix A: the relationship between the relaxation function and the conductivity of defects

Let us consider a homogeneous, isotropic dielectric in a charged capacitor with an electric field $\mathbf{E}_{ex}(\mathbf{r})$. This field is considered as external to the dielectric. We have defined the dielectric sample in our model as a dipole system with charge carriers. Our model also suggests that the jumping of charge carriers from one water molecule (which acts as a dipole unit of the system) to another leads to a change in the direction of its dipole moments and, as a consequence, to a change in the total polarization of the sample. We now consider only one type of charge carrier and later generalize for several types.

If the dielectric is under the influence of a static external electric field, $\mathbf{E}_{ex}(\mathbf{r})$, over a long time period, it reaches the equilibrium state with some stationary distribution of charge carriers $\rho(\mathbf{r})$. This distribution in the static case obeys the Boltzmann distribution, with potential $U(\mathbf{r}) \sim \phi(\mathbf{r})$, where $\nabla\cdot\phi(\mathbf{r}) = \mathbf{E}_{ex}(\mathbf{r})$, and it can be described by the well-known Poisson–Boltzmann equation in a thermodynamic equilibrium state.[43] However, if we switch off the external field $\mathbf{E}_{ex}(\mathbf{r})$ at the moment $t = 0$, the distribution of charge carriers $\rho(\mathbf{r})$ thus created becomes in itself a source of some field $\mathbf{E}_c(\mathbf{r})$ that is defined by equation $\nabla\cdot\mathbf{E}_c(\mathbf{r}) = \rho(\mathbf{r})/\varepsilon_0$. In turn, the field $\mathbf{E}_c(\mathbf{r})$ affects the charge carriers and changes the distribution density $\rho(\mathbf{r})$. Therefore, we have a non-static case and $\mathbf{E}_c(\mathbf{r})$ and $\rho(\mathbf{r})$ should be defined as functions of time: $\mathbf{E}_c(\mathbf{r}) \rightarrow \mathbf{E}_c(t,\mathbf{r})$ and $\rho(\mathbf{r}) \rightarrow \rho(t,\mathbf{r})$. Then, assuming that there are no external charges $\rho_{ext} = 0$, *i.e.*, the total charge of the medium is zero, we can write that

$$\nabla\cdot\mathbf{E}_c(t,\mathbf{r}) = \rho(t,\mathbf{r})/\varepsilon_0, \tag{A1}$$

here, $\varepsilon_0 = 8.854 \times 10^{-12}$ F m^{-1} is the vacuum permittivity. In turn, from the linear response theory, the polarization $P(t,\mathbf{r})$ at time t at point $\mathbf{r}$ can be written as

$$\begin{aligned}\mathbf{P}(t,\mathbf{r}) &= \mathbf{P}(0,\mathbf{r}) - \varepsilon_0\chi\int_0^t \mathrm{d}t'\int_{\Delta V}\mathrm{d}V' f_p(\mathbf{r}-\mathbf{r}', t-t')\mathbf{E}_c(t',\mathbf{r}') \\ &= \mathbf{P}(0,\mathbf{r}) - \varepsilon_0\chi\int_0^t \mathrm{d}t' f_p(t-t')\mathbf{E}_c(t',\mathbf{r}),\end{aligned} \tag{A2}$$

where $\mathbf{P}(0,\mathbf{r})$ is the initial polarization. Here, we have neglected the spatial dispersion and imply a localized response of the material, *i.e.*, $f_p(t,\mathbf{r}) = f_p(t)\delta(\mathbf{r})$, where $f_p(t)$ is a pulse-response function of the polarization.[44] Note that the polarization $\mathbf{P}(t,\mathbf{r})$ in eqn (A2) includes the polarization $\mathbf{P}_s(t,\mathbf{r})$ caused by the separation of charge carriers within the sample and the polarization $\mathbf{P}_d(t,\mathbf{r})$ caused by ordering of the dipole moments in the system, *i.e.* $\mathbf{P}(t,\mathbf{r}) = \mathbf{P}_s(t,\mathbf{r}) + \mathbf{P}_d(t,\mathbf{r})$. In the absence of external charges, $\rho_{ext} = 0$. Thus, for the overall polarization, we can write

$$\nabla\cdot\mathbf{P}(t,\mathbf{r}) = -\rho(t,\mathbf{r}). \tag{A3}$$

The created field, $\mathbf{E}_c(t,\mathbf{r})$, in turn induces a current of charge carriers. As noted in our model above, the translation motion of the charge carriers, besides changing $\mathbf{P}_s(t,\mathbf{r})$, is also accompanied by the rotation of the molecular dipoles, *i.e.* changing $\mathbf{P}_d(t,\mathbf{r})$. We can describe the induced current as the time derivative of the total polarization $\mathbf{P}(t,\mathbf{r}) = \mathbf{P}_s(t,\mathbf{r}) + \mathbf{P}_d(t,\mathbf{r})$, *i.e.*, $j = \partial\mathbf{P}(t,\mathbf{r})/\partial t$. From eqn (A2), we have

$$\mathbf{j}(t,\mathbf{r}) = -\varepsilon_0\chi f_p(0)\mathbf{E}_c(t,\mathbf{r}) + \int_0^t \sigma_c(t-t')\mathbf{E}_c(t',\mathbf{r})\mathrm{d}t', \tag{A4}$$

where we denote $\sigma_c(t) = -\varepsilon_0\chi\partial f_p(t)/\partial t$. A Fourier-transformed $\sigma_c(t)$ defines the frequency-dependent complex conductivity, $\sigma_c^*(\omega)$, of the charge carriers. Remember that in terms of our model, the conductivity obtained is defined only by the transfer of protons from one molecule to another in the case of ionic defects, or by the migration of L–D defects. Also, from the initial condition $\mathbf{j}(0,\mathbf{r}) = 0$ we find that $f_p(0) = 0$. Under this condition we imply that at the moment the external field $\mathbf{E}_{ex}(\mathbf{r})$ is switched off, we have a stationary equilibrium system, *i.e.* the charge carriers (H_3O^+/OH^- or L–D pair defects) are at rest and their current is absent.

The conservation of the charge carriers is expressed by the continuity equation $\partial\rho(t,\mathbf{r})/\partial t + \nabla\cdot\mathbf{j}(t,\mathbf{r}) = 0$. Substituting $\mathbf{j}(t,\mathbf{r})$ from eqn (A4) (with condition $f_p(0) = 0$), and then taking ∇ under the time integration and using eqn (A1), we have

$$\frac{\partial}{\partial t}\rho(t,\mathbf{r}) + \frac{1}{\varepsilon_0}\int_0^t \sigma_c(t-t')\rho(t',\mathbf{r})\mathrm{d}t' = 0. \tag{A5}$$

By one-sided Fourier transform of eqn (A5) we find that

$$i\omega\cdot\rho^*(\omega,\mathbf{r}) - \rho(0,\mathbf{r}) + \frac{1}{\varepsilon_0}\sigma_c^*(\omega)\rho^*(\omega,\mathbf{r}) = 0, \tag{A6}$$

where $\rho(0,\mathbf{r})$ is the density of the charges at time $t = 0$. From eqn (A6) we find that

$$\begin{aligned}\rho^*(\omega,\mathbf{r}) &= \frac{\rho(0,\mathbf{r})}{i\omega + \sigma_c^*(\omega)/\varepsilon_0} = \rho(0,\mathbf{r})\gamma^*(\omega), \\ \gamma^*(\omega) &= \frac{1}{i\omega + \sigma_c^*(\omega)/\varepsilon_0}.\end{aligned} \tag{A7}$$

Thus, $\rho^*(\omega,\mathbf{r})$ is a separate function of variables $\mathbf{r}$ and ω. In turn, from eqn (A3) we find that the function $\mathbf{P}(t,\mathbf{r})$ is also a separate function, $\mathbf{P}(t,\mathbf{r}) = \mathbf{P}_r(\mathbf{r})\mathbf{P}(t)$. We can thus conclude that

$$\frac{\rho(t,\mathbf{r})}{\rho(0,\mathbf{r})} = \frac{\nabla\cdot\mathbf{P}(t,\mathbf{r})}{\nabla\cdot\mathbf{P}(0,\mathbf{r})} = \frac{P(t)\nabla\cdot\mathbf{P}_r(\mathbf{r})}{P(0)\nabla\cdot\mathbf{P}_r(\mathbf{r})} = \phi(t). \tag{A8}$$

From eqn (A7) and (A8) it follows that the relaxation function

$$\phi^*(\omega) = \frac{1}{i\omega + \sigma_c^*(\omega)/\varepsilon_0}. \quad \text{(A9)}$$

If we consider N types of charge carriers we can rewrite eqn (A9) as

$$\phi^*(\omega) = \frac{1}{i\omega + \sum_{i=1}^{N} \sigma_c^{*i}(\omega)/\varepsilon_0}, \quad \text{(A10)}$$

where $\sigma_c^{*i}(\omega)$ denotes i-types of charge carriers. It is assumed that different types of carriers are not correlated to each other.

Finally, we should note that the defined conductivity $\sigma_c^*(\omega)$ is not the total macroscopic AC conductivity $\sigma^*(\omega)$ that is related to the complex dielectric permittivity by $\sigma^*(\omega) = i\omega\varepsilon_0\varepsilon^*(\omega)$. The relationship between them can be found in ref. 45.

Mathematical appendix B: analysis of the complex dielectric permittivity function

Let us consider the equation for the normalized complex dielectric permittivity (NCDP)

$$\bar{\varepsilon}(\omega) = \frac{\varepsilon^*(\omega) - \varepsilon_\infty}{\varepsilon_s - \varepsilon_\infty} = \frac{1}{1 + [(i\omega\tau_1)^{-\alpha_1} + (i\omega\tau_2)^{-\alpha_2}]^{-1}}. \quad \text{(B1)}$$

Using addition formulas of complex numbers in the exponential form, we can reduce this equation to the Cole–Cole law with frequency-dependent parameters

$$\bar{\varepsilon}(\omega) = \frac{1}{1 + (i\omega\tau(\omega))^{\alpha(\omega)}}, \quad \text{(B2)}$$

where $\alpha = \alpha(\omega)$ and $\tau = \tau(\omega)$ are defined by

$$(\omega\tau)^{-\alpha} = \sqrt{(\omega\tau_1)^{-2\alpha_1} + (\omega\tau_2)^{-2\alpha_2} + 2(\omega\tau_1)^{-\alpha_1}(\omega\tau_2)^{-\alpha_2}\cos\left(\frac{\pi}{2}[\alpha_1 - \alpha_2]\right)}, \quad \text{(B3)}$$

$$\operatorname{tg}\left(\frac{\pi\alpha}{2}\right) = \frac{\tau_1^{-\alpha_1}\sin(\pi\alpha_1/2) + \tau_2^{-\alpha_2}\sin(\pi\alpha_2/2)\omega^{\alpha_1-\alpha_2}}{\tau_1^{-\alpha_1}\cos(\pi\alpha_1/2) + \tau_2^{-\alpha_2}\cos(\pi\alpha_2/2)\omega^{\alpha_1-\alpha_2}}. \quad \text{(B4)}$$

In the general case, eqn (B1) or (B2) can produce two loss peaks in a frequency domain. It is obvious that in the trivial case where $\alpha_1 = \alpha_2 \equiv \alpha$, then

$$\tau = (\tau_1^{-\alpha} + \tau_2^{-\alpha})^{-1/\alpha},$$

and eqn (B1) leads to the standard Cole–Cole law with one loss peak. It is necessary to define the conditions where eqn (B2) can be applied to fit dielectric spectra with one loss peak.

With a small difference between α_1 and α_2, *i.e.* $\Delta\alpha = |\alpha_1 - \alpha_2|/2 \ll 1$, we can expand eqn (B4) as a series in $\Delta\alpha$

$$\alpha \approx \alpha_0 + \frac{\tau_1^{-\alpha_0} - \tau_2^{-\alpha_0}}{\tau_1^{-\alpha_0} + \tau_2^{-\alpha_0}}\Delta\alpha = \frac{\alpha_1\tau_1^{-\alpha_0} + \alpha_2\tau_2^{-\alpha_0}}{\tau_1^{-\alpha_0} + \tau_2^{-\alpha_0}}, \quad \alpha_0 = \frac{\alpha_1 + \alpha_2}{2}. \quad \text{(B5)}$$

As we can see from eqn (B5) the parameter α does not depend on frequency in the linear case of $\Delta\alpha$. The expression for parameter τ in a linear approximation of $\Delta\alpha$ can be obtained by the logarithm of eqn (B3) and expansion of its right-part as a series in $\Delta\alpha$. As a result, we get

$$\alpha\ln\tau \approx \alpha_0\ln\tau_0 + \frac{\tau_1^{-\alpha_0}\ln\tau_1 - \tau_2^{-\alpha_0}\ln\tau_2}{\tau_1^{-\alpha_0} + \tau_2^{-\alpha_0}}\Delta\alpha, \quad \text{(B6)}$$

where

$$\tau_0 = (\tau_1^{-\alpha_0} + \tau_2^{-\alpha_0})^{-1/\alpha_0} \quad \text{(B7)}$$

From eqn (B6) we obtain (in a linear approximation)

$$\tau = \tau_0\left[1 + \left\{\left(\frac{\tau_1}{\tau_0}\right)^{-\alpha_0}\ln(\tau_1/\tau_0) + \left(\frac{\tau_2}{\tau_0}\right)^{-\alpha_0}\ln(\tau_0/\tau_2)\right\}\frac{\Delta\alpha}{\alpha_0}\right] = \tau_0\left[1 + \frac{\alpha - \alpha_2}{2\alpha_0}\ln(\tau_1/\tau_0) + \frac{\alpha - \alpha_1}{2\alpha_0}\ln(\tau_2/\tau_0)\right]. \quad \text{(B8)}$$

Therefore, the parameter τ, in a linear approximation of $\Delta\alpha$, also does not depend on frequency.

Acknowledgements

The authors of this paper express their deep thanks to Prof. Naoki Shinyashiki for making available the use of their reliable data for verification of these theoretical results. The authors are grateful to Prof. V. Ilyin for valuable discussions. The work was supported by the Valazzi-Pikovsky Fellowship (Lady Davis Fellowship).

References

1 N. Grishina and V. Buch, *J. Chem. Phys.*, 2004, **120**, 5217.
2 B. Geil, T. M. Kirschgen and F. Fujara, *Phys. Rev. B: Condens. Matter Mater. Phys.*, 2005, **72**, 014304.
3 P. V. Hobbs, *Ice Physics*, Clarendon Press, Oxford, 1974, p. 837.
4 D. Eisenberg and W. Kauzmann, *The structure and properties of water*, OUP Oxford, 2005, p. 235.
5 G. Malenkov, *J. Phys.: Condens. Matter*, 2009, **21**, 283101.
6 V. F. Petrenko and R. W. Whitworth, *Physics of ice*, Clarendon Press, Oxford, 1999, p. 386.
7 D. K. Lonsdale, The Structure of Ice, *Proc. R. Soc. London, Ser. A*, 1958, 434.
8 J. D. Bernal and R. H. Fowler, *J. Chem. Phys.*, 1933, **1**, 515.
9 L. Pauling, *J. Am. Chem. Soc.*, 1935, **57**, 2680.
10 R. P. Auty and R. H. Cole, *J. Chem. Phys.*, 1952, **20**, 1309.
11 A. Steinemann, *Helv. Phys. Acta*, 1957, **30**, 581.
12 S. R. Gough and D. W. Davidson, *J. Chem. Phys.*, 1970, **52**, 544.

13 O. Worz and R. H. Cole, *J. Chem. Phys.*, 1969, **51**, 1546.
14 R. Ruepp, in *Physics and Chemistry of Ice*, ed. E. Whalley, S. J. Jones and L. W. Gold, Royal Society of Canada, Ottawa, 1973, p. 179.
15 G. P. Johari and S. J. Jones, *Proc. R. Soc. London, Ser. A*, 1976, **349**, 467.
16 G. P. Johari and E. Whalley, *J. Chem. Phys.*, 1981, **75**, 1333.
17 N. Shinyashiki, *et al.*, *J. Phys. Chem. B*, 2009, **113**, 14448.
18 G. P. Johari and S. J. Jones, *J. Glaciol.*, 1978, **21**, 259.
19 A. Hippel, *IEEE Trans. Electr. Insul.*, 1988, **23**(5), 825.
20 J. H. Bilgram and H. Granicher, *Phys. Cond. Matter*, 1974, **18**, 27.
21 A. Melinder, *Int. J. Refrig.*, 2010, **33**, 150.
22 N. Bjerrum, *K. Dan. Vidensk. Selsk., Mat.-Fys. Medd.*, 1951, **27**, 1.
23 N. Bjerrum, *Science*, 1952, **115**, 38.
24 R. Podeszwa and V. Buch, *Phys. Rev. Lett.*, 1999, **83**, 22.
25 M. de Koning, *et al.*, *Phys. Rev. Lett.*, 2006, **97**, 155501.
26 K. Mochizuki, M. Matsumoto and I. Ohmine, *Nature*, 2013, **498**, 350.
27 N. Agmon, *Chem. Phys. Lett.*, 1995, **244**, 45.
28 R. Pfeifer and H. G. Hertz, *Ber. Bunsen-Ges.*, 1990, **94**, 134.
29 R. A. Robinson and R. H. Stokes, *Electrolyte solutions*, Butterworths, London, 2nd edn, 1959.
30 G. P. Johari and E. Whalley, *J. Chem. Phys.*, 2001, **115**, 3274.
31 B. Roling, C. Martiny and S. Bruckner, *Phys. Rev. B: Condens. Matter Mater. Phys.*, 2001, **63**, 214203.
32 Y. Gefen, A. Aharony and S. Alexander, *Phys. Rev. Lett.*, 1983, **50**, 77.
33 R. Metzler, E. Barkai and J. Klafter, *Physica A*, 1999, **266**, 343.
34 R. Metzler, J. Klafter and I. M. Sokolov, *Phys. Rev. E: Stat. Phys., Plasmas, Fluids, Relat. Interdiscip. Top.*, 1998, **58**, 1621.
35 Yu. P. Kalmykov, S. V. Titov and W. T. Coffey, *Phys. Rev. E: Stat., Nonlinear, Soft Matter Phys.*, 2012, **85**, 041101.
36 W. T. Coffey, Yu. P. Kalmykov and S. V. Titov, *Eur. Phys. J.: Spec. Top.*, 2013, **222**, 1847.
37 K. Weron, *et al.*, *Proc. R. Soc. A*, 2012, **468**, 1615–1628.
38 I. I. Popov, R. R. Nigmatullin and A. A. Khamzin, *J. Non-Cryst. Solids*, 2012, **358**, 1516.
39 R. Hilfer, *Physica A*, 1995, **221**, 8.
40 R. Hilfer, *Fractals*, 1995, **3**, 54.
41 R. Hilfer, in *Fractional time evolution Applications of Fractional Calculus in Physics*, ed. R. Hilfer, World Scientific, Singapore, 2000, p. 87.
42 N. Shinyashiki, (private communication).
43 F. Fogolari, A. Brigo and H. Molinari, *J. Mol. Recognit.*, 2002, **15**(6), 377.
44 C. J. F. Boettcher and P. Bordewijk, *Theory of Electric Polarization*, Elsevier, Amsterdam, 2nd edn, 1992, vol. 2.
45 A. A. Khamzin, I. I. Popov and R. R. Nigmatullin, *Phys. Rev. E: Stat., Nonlinear, Soft Matter Phys.*, 2014, **89**, 032303.